Supporting Information

Evaluation of fluoride adsorptive removal by metallic phosphates

Ruijie Wang, Yingpeng Gu, Mengfei Ma, Yue Sun*

Department of Municipal Engineering, School of Civil Engineering, Southeast University, Nanjing, 210096, China

* Corresponding author at: School of Civil Engineering, Southeast University, Nanjing 210096, China.

E-mail address: sycyseu@163.com (Y. Sun).

Number of Pages: 18

Number of Figures: 7

Number of Tables: 7

List of Figures and Tables

Figure S1. The optimal molar ratio of metal and phosphoru in the synthesis of metallic phosphates.

Figure S2. Nitrogen adsorption-desorption isotherms of adsorbents.

Figure S3. Isoelectric points of adsorbents.

Figure S4. Effect of equilibrium pH after adsorption on fluoride adsorption onto the adsorbents.

Figure S5. Adsorption isotherms of fluoride onto the adsorbents at different temperatures.

Figure S6. Desorption capacity of fluoride onto the adsorbents in different concentrations of NaOH.

Figure S7. Adsorption capacity of fluoride by adsorbents in five static adsorption-desorption cycle experiments with actual wastewater.

Table S1. Primary properties of adsorbents.

Table S2. Adsorption kinetic fitting parameters of adsorbents.

Table S3. Adsorption isotherm fitting parameters of adsorbents.

Table S4. Coordination constants of metal and fluoride.

Table S5. The adsorption properties of various mono- or polymetallic-based adsorbents.

Table S6. Adsorption thermodynamic fitting parameters of adsorbents.

Table S7. The water quality parameters of actual photovoltaic wastewater.

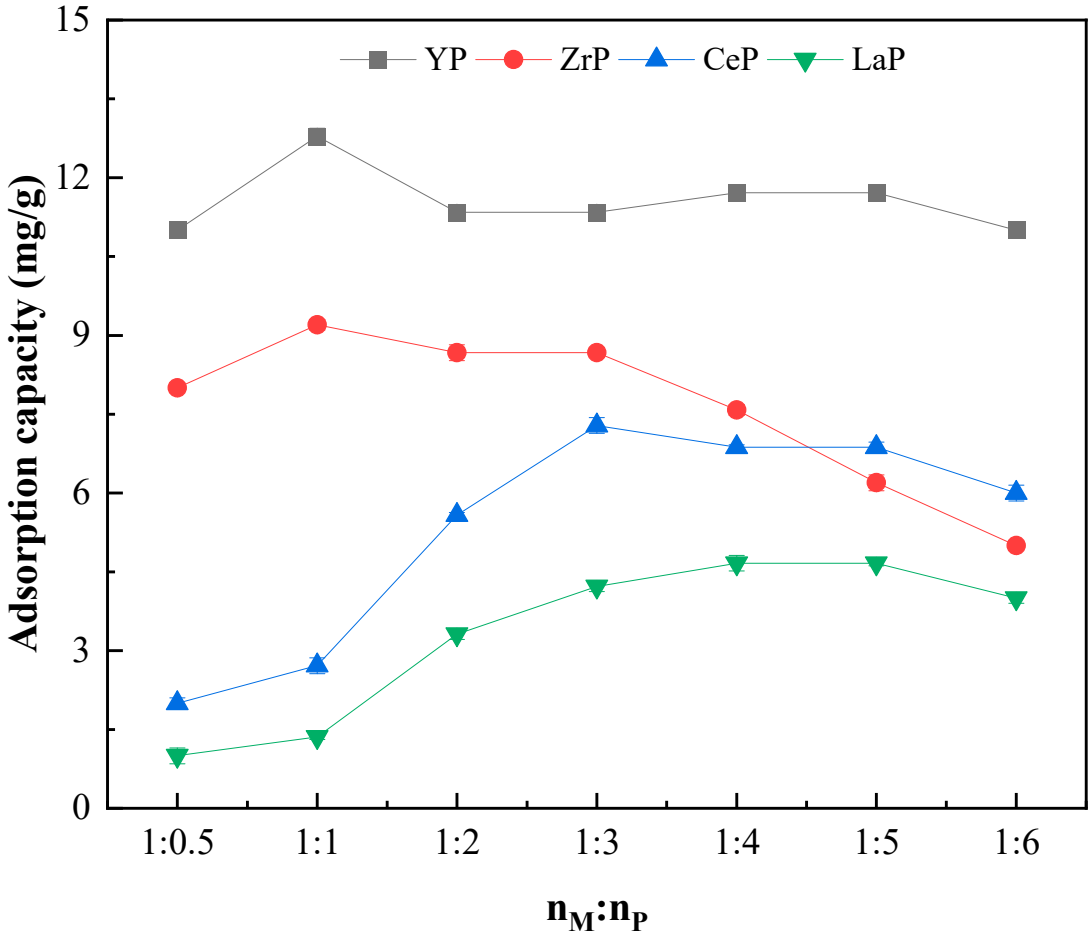


Figure S1. The optimal molar ratio of metal and phosphoru in the synthesis of metallic phosphates.

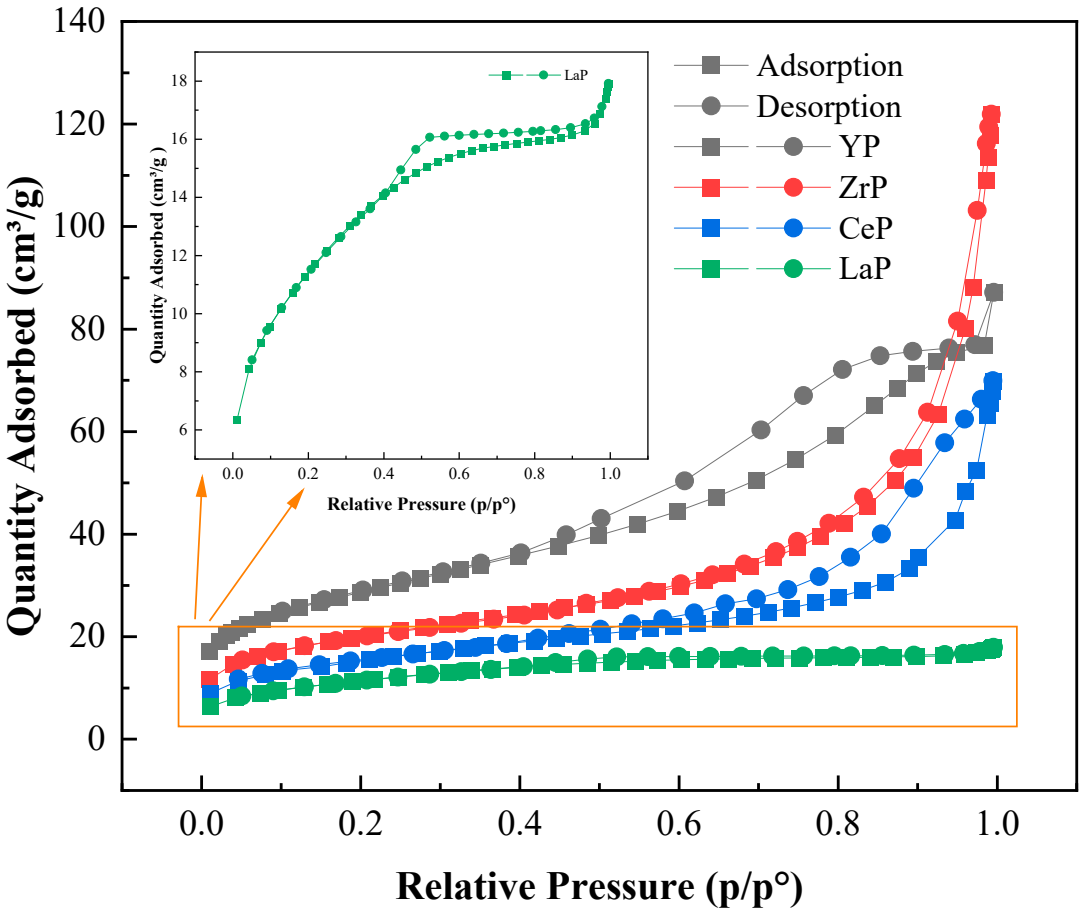


Figure S2. Nitrogen adsorption-desorption isotherms of adsorbents.

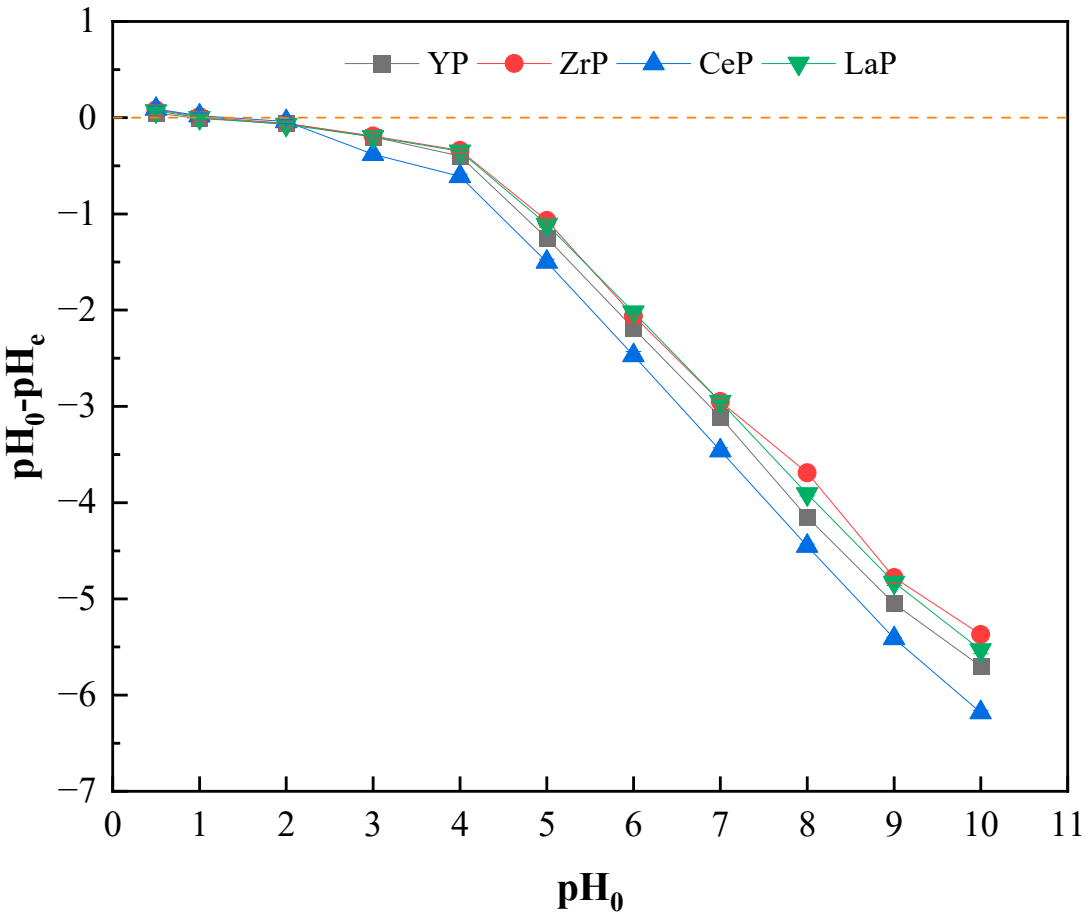


Figure S3. Isoelectric points of adsorbents.

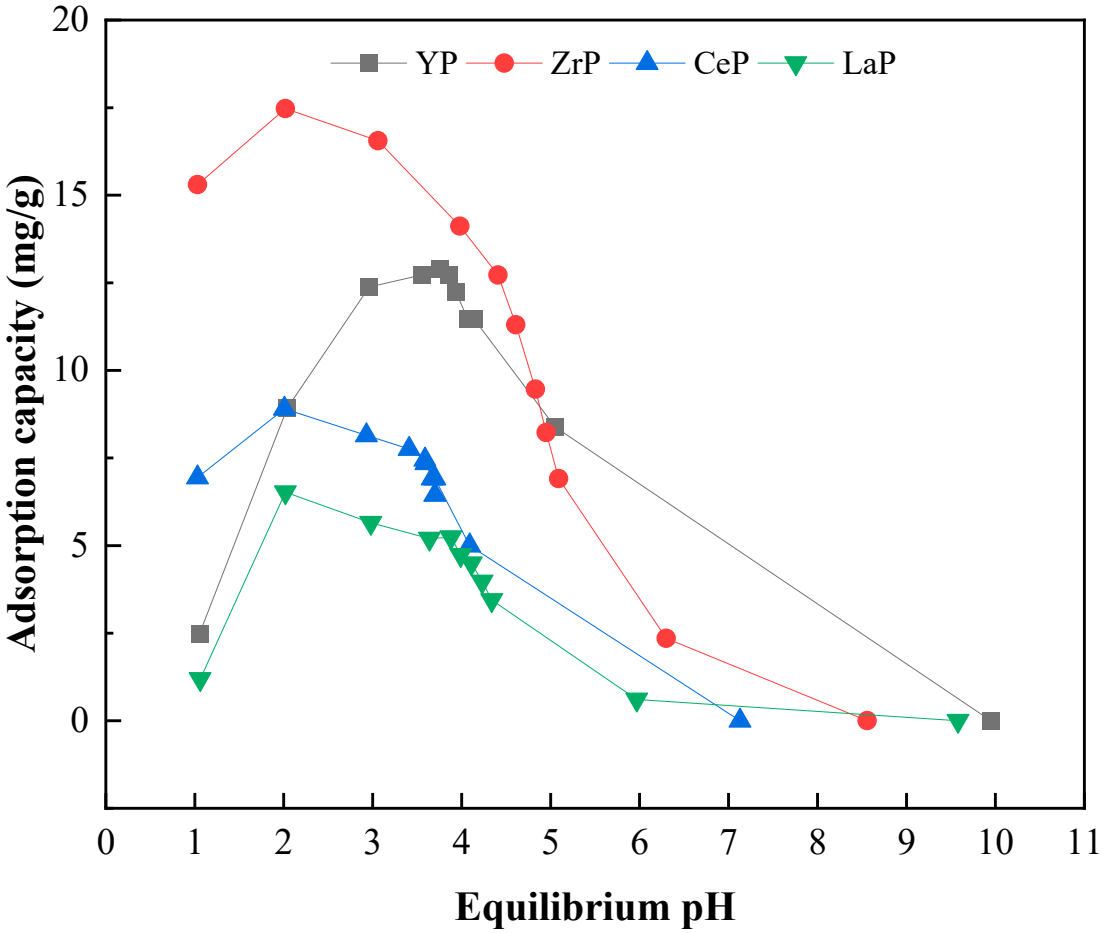
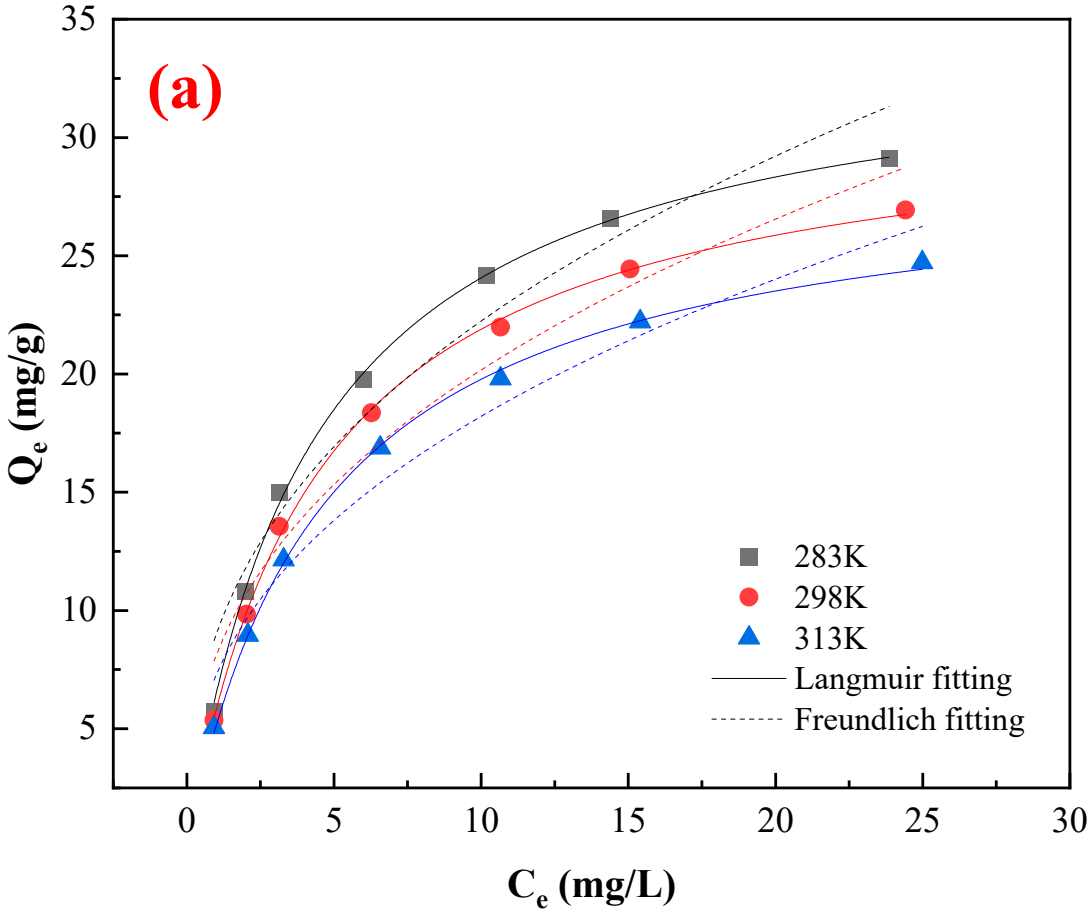
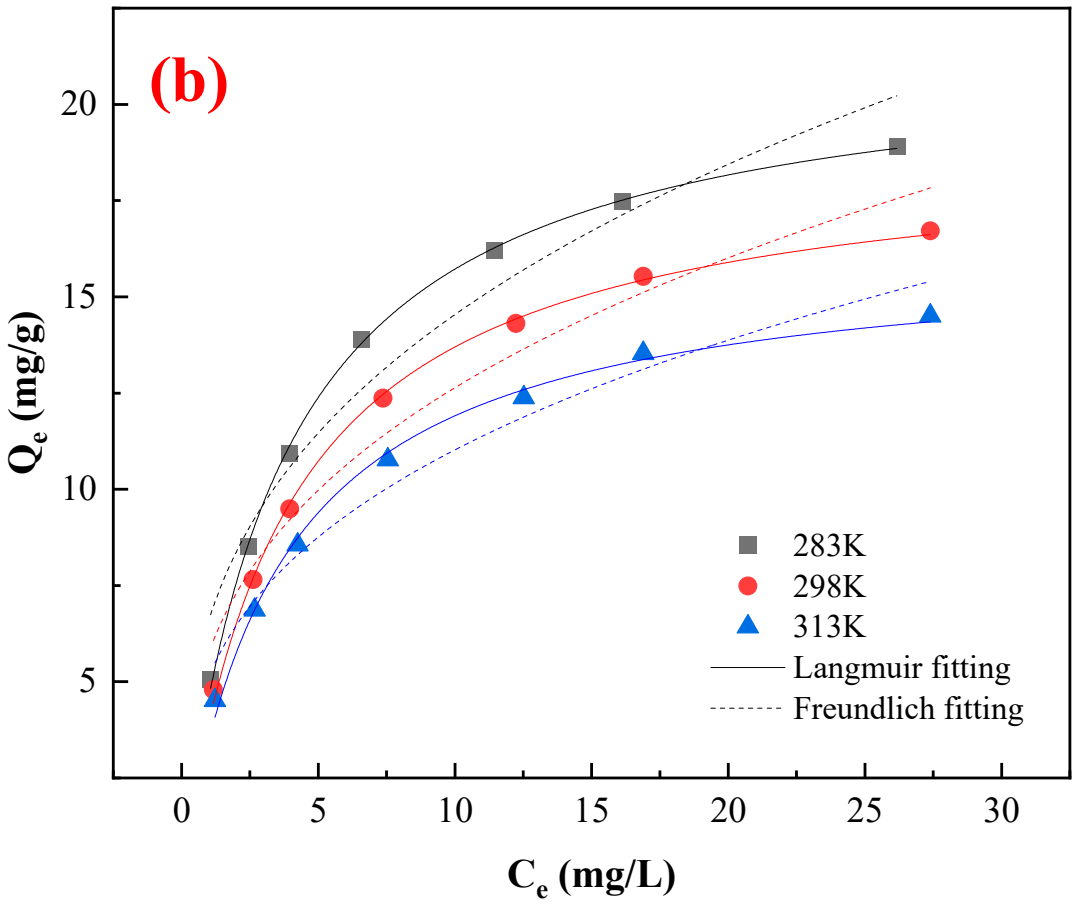
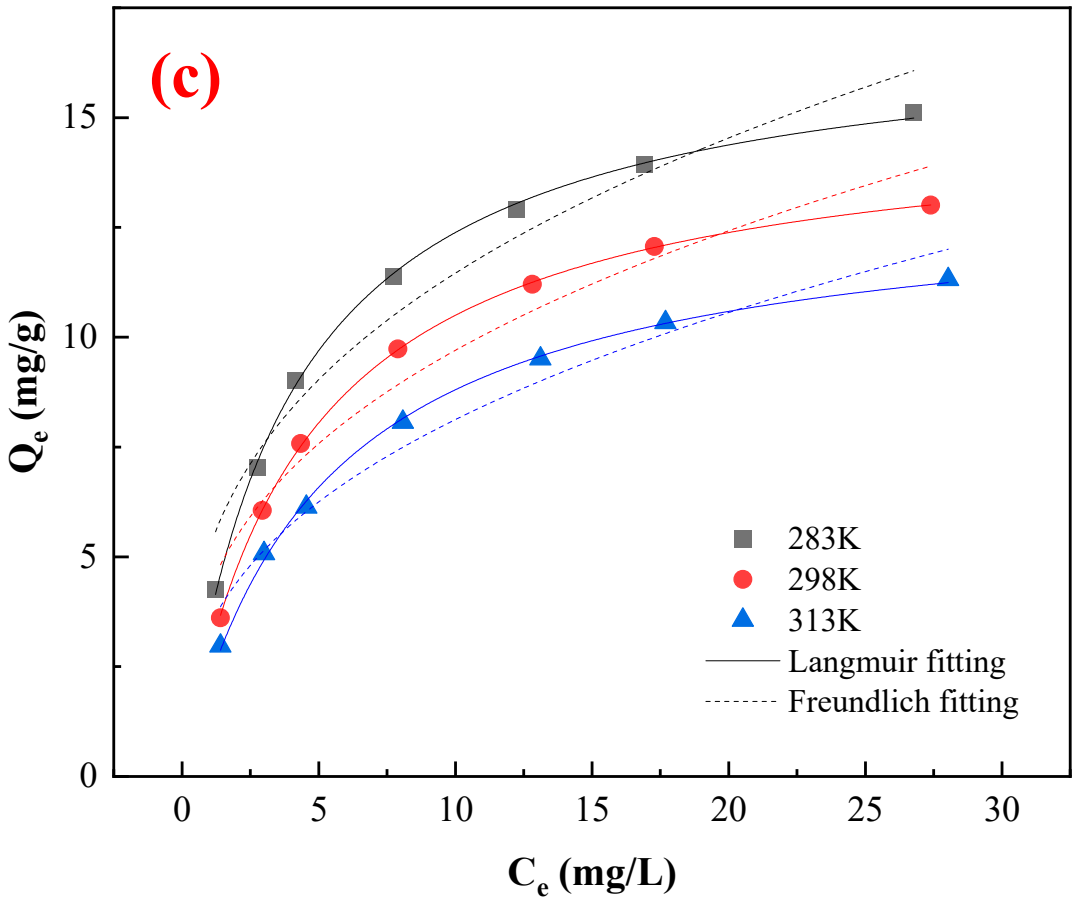


Figure S4. Effect of equilibrium pH after adsorption on fluoride adsorption onto the adsorbents (Reaction conditions: T = 298 K, pH = 6.8±0.2, initial fluoride = 5 mg/L, and adsorbent dosage = 0.20 g/L).


(a)
35
30
25
20
15
10
5
0
5
10
15
20
25
30
Q_e (mg/g)
C_e (mg/L)
283K
298K
313K
Langmuir fitting
Freundlich fitting


(b)
20
15
10
5
0
5
10
15
20
25
30
Q_e (mg/g)
C_e (mg/L)
283K
298K
313K
Langmuir fitting
Freundlich fitting


(c)
15
10
5
0
0
5
10
15
20
25
30
Q_e (mg/g)
C_e (mg/L)
283K
298K
313K
Langmuir fitting
Freundlich fitting

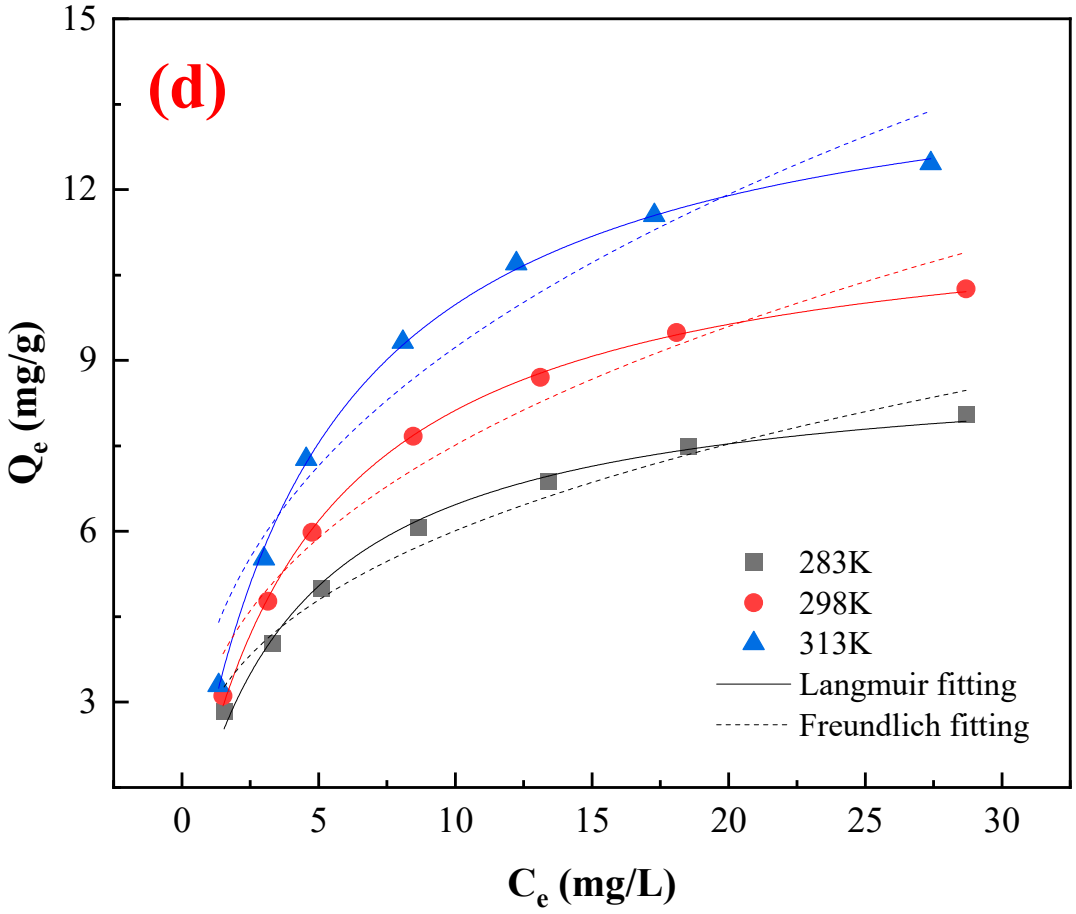


Figure S5. Adsorption isotherms of fluoride onto the adsorbents at different temperatures.(a) YP. (b) ZrP. (c) CeP. (d) LaP. ((Reaction conditions: pH = 6.8±0.2, and adsorbent dosage = 0.20 g/L).

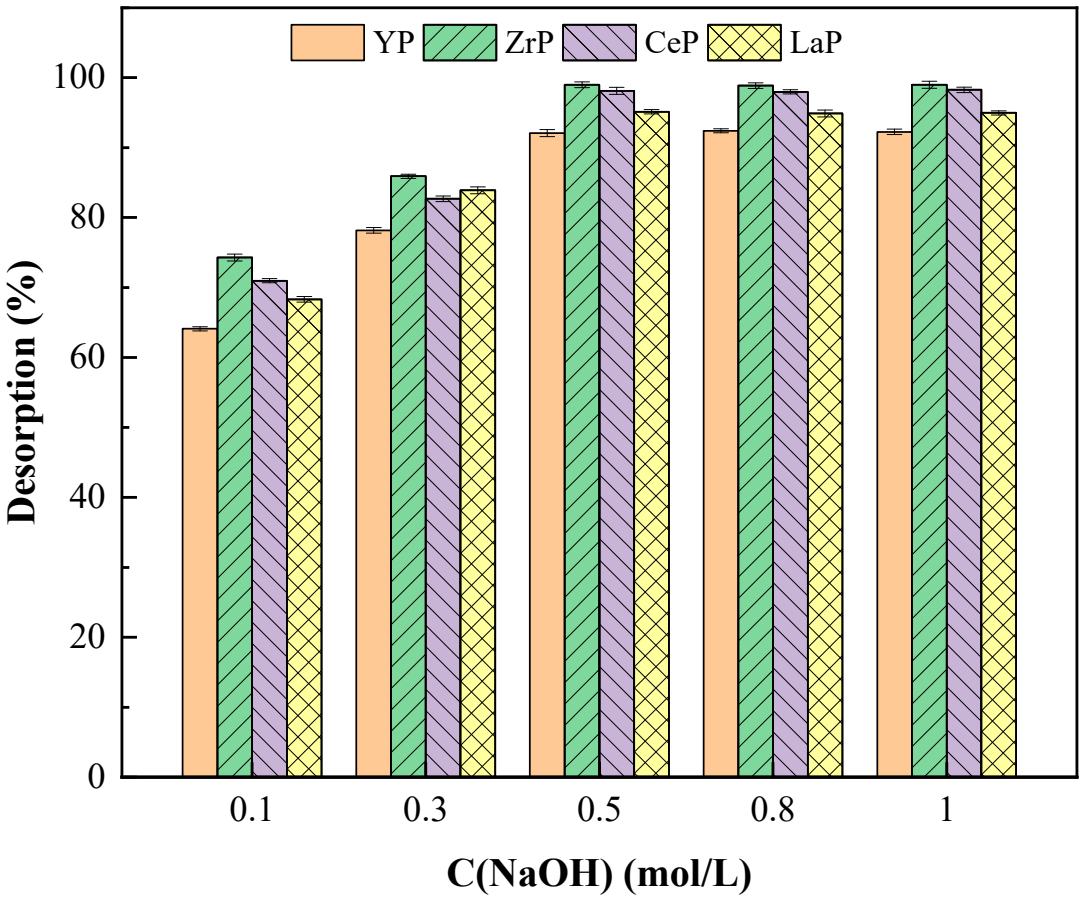


Figure S6. Desorption capacity of fluoride onto the adsorbents in different concentrations of NaOH.

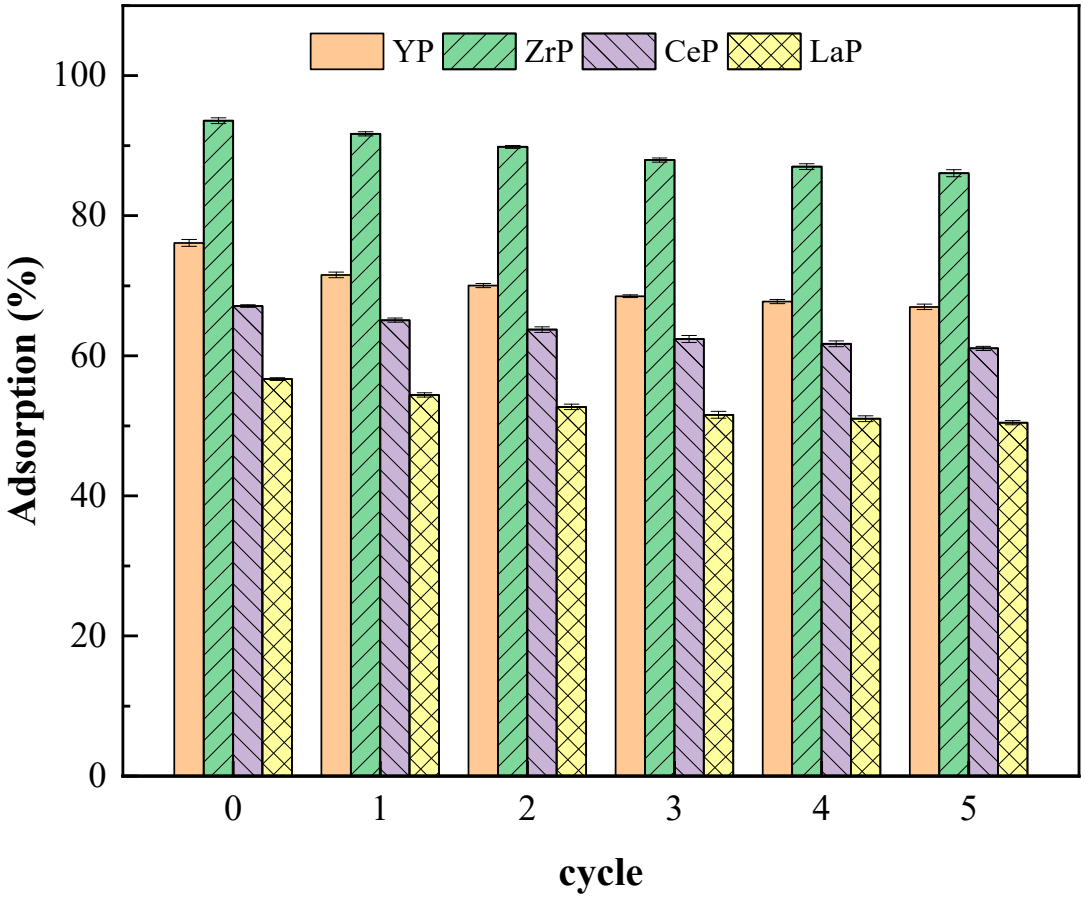


Figure S7. Adsorption capacity of fluoride by adsorbents in five static adsorption-desorption cycle experiments with actual wastewater. (Reaction conditions: adsorbent dosage = 1.0 g/L, T = 298 K)

Table S1. Primary properties of adsorbents.

Adsorbents	Content of metal ion	Content of phosphoru	M:P	Major composition	BET surface area	Average pore diameter	Average pore volume
	mmol/g	mmol/g	/	/	m^2/g	nm	cm^3/g
YP	3.650	4.327	1:1.19	YPO_4	102.90	5.06	0.108
ZrP	0.724	1.707	1:2.35	$Zr(HPO_4)_2$	70.21	14.27	0.187
CeP	1.287	5.017	1:3.39	$CePO_4$ and $Ce(HPO_4)_2$	51.84	7.69	0.092
LaP	3.134	4.529	1:1.44	$LaPO_4$	40.66	3.11	0.027

Table S2. Adsorption kinetic fitting parameters of adsorbents.

Adsorbents	Pseudo-first-order					Pseudo-second-order			
	$Q_{e.exp}$	$Q_{e.cal}$	k_1	${R_1}^2$	SSE	$Q_{e.cal}$	k_2	${R_2}^2$	SSE
	mg/g	mg/g	1/min			mg/g	g/(mg·min)		
YP	12.82	12.51	0.173	0.970	4.814	12.91	0.025	0.999	0.202
ZrP	9.56	9.24	0.047	0.972	3.537	9.86	0.008	0.999	0.065
CeP	7.67	7.49	0.055	0.968	2.556	7.94	0.011	0.998	0.195
LaP	4.79	4.65	0.136	0.965	0.823	4.83	0.048	0.999	0.030

Table S3. Adsorption isotherm fitting parameters of adsorbents.

Adsorbents	T	Langmuir				Freundlich		
		Q_m	K_L	R_L	R_1^2	$1/n$	K_F	R_2^2
		mg/g	L/mg				mg/g $\cdot (L/mg)^{\frac{1}{n}}$	

	283K	34.43	0.232	0.126	0.999	0.394	8.983	0.941
YP	298K	31.61	0.225	0.129	0.999	0.396	8.096	0.950
	313K	28.98	0.215	0.134	0.999	0.399	7.267	0.958
	283K	21.52	0.271	0.110	0.999	0.343	6.596	0.940
ZrP	298K	18.94	0.261	0.113	0.998	0.341	5.757	0.950
	313K	16.27	0.253	0.116	0.995	0.332	5.133	0.958
	283K	17.14	0.261	0.113	0.999	0.343	5.201	0.945
CeP	298K	15.09	0.229	0.127	0.999	0.357	4.268	0.940
	313K	13.28	0.197	0.145	0.999	0.379	3.398	0.958
	283K	9.03	0.253	0.116	0.992	0.369	3.949	0.936
LaP	298K	11.84	0.219	0.132	0.999	0.353	3.332	0.952
	313K	14.72	0.211	0.136	0.999	0.329	2.835	0.966

Table S4. Coordination constants of metal and fluoride.

Metal	Y	Zr	Ce	La
Coordination constant	4.81	8.80	7.57	2.77

Table S5. The adsorption properties of various mono- or polymetallic-based adsorbents.

Meterials	Conditions	Q_{max} (mg/g)	References
Iron(III)-zirconium(IV) hybrid oxide	pH=6.8; T=303K	8.21	[1]
Granular ferric hydroxide (GFH)	pH=6.0-7.0;	7.00	[2]

	T=279K		
Granular zirconium–iron oxide (GZI)	pH=6.0; T=298K	22.23	[3]
Mg-Al-Zr triple-metal composite	pH=7.0; T=298K	22.90	[4]
Manganese-oxide-coated alumina	pH=7.0; T=303K	2.85	[5]
CeO2-Cubes	pH=3.5; T=298K	7.00	[6]
Mg–Al–Fe hydrotalcite	pH=6.0; T=298K	14.92	[7]
AZrP	Not related	2.64	[8]
Lanthanum-carbon hybrid adsorbent	pH=7; T=298K	8.1	[9]
Zr-La/PP composites	pH=7	16.5	[10]
HAP microsphere	pH=7	14.3	[11]
MgO-Fe2O3 nanoparticles	pH=6; T=301K	10.96	[12]
YP	pH=6.8±0.2；T=283K	34.43	This study
ZrP	pH=6.8±0.2；T=283K	21.52	This study
CeP	pH=6.8±0.2；T=283K	17.14	This study
LaP	pH=6.8±0.2；T=313K	14.72	This study

Table S6. Adsorption thermodynamic fitting parameters of adsorbents.

Adsorbents	T	ΔH kJ/mol	ΔS J/mol·K	ΔG kJ/mol	R^2
YP	283K	-5.144	40.933	-16.721	0.995
	298K			-17.357	
	313K			-17.947	
ZrP	283K	-7.658	27.659	-15.491	0.999
	298K			-15.890	
	313K			-16.322	
CeP	283K	-8.250	23.539	-14.910	0.999
	298K			-15.269	
	313K			-15.615	
LaP	283K	11.804	88.557	-13.266	0.998
	298K			-14.566	
	313K			-15.925	

Table S7. The water quality parameters of actual photovoltaic wastewater.

pH	F^-	Cl^-	SO_4^{2-}	NO_3^-	Ca^{2+}	Mg^{2+}	Al^{3+}	COD
	(mg/L)	(mg/L)	(mg/L)	(mg/L)	(mg/L)	(mg/L)	(mg/L)	(mg/L)
6.5	4.96	337.7	123.6	136.2	103.5	31.1	6.6	74

References

1. Biswas, K.; Bandhoyapadhyay, D.; Ghosh, U.C. Adsorption Kinetics of Fluoride on Iron(III)-Zirconium(IV) Hybrid Oxide. *Adsorption* **2007**, *13*, 83–94, doi:10.1007/s10450-007-9000-1.
2. Kumar, E.; Bhatnagar, A.; Ji, M.; Jung, W.; Lee, S.-H.; Kim, S.-J.; Lee, G.; Song, H.; Choi, J.-Y.; Yang, J.-S.; et al. Defluoridation from Aqueous Solutions by Granular Ferric Hydroxide (GFH). *Water Res.* **2009**, *43*, 490–498, doi:10.1016/j.watres.2008.10.031.
3. Dou, X.; Zhang, Y.; Wang, H.; Wang, T.; Wang, Y. Performance of Granular Zirconium–Iron Oxide in the Removal of Fluoride from Drinking Water. *Water Res.* **2011**, *45*, 3571–3578, doi:10.1016/j.watres.2011.04.002.
4. Wang, M.; Yu, X.; Yang, C.; Yang, X.; Lin, M.; Guan, L.; Ge, M. Removal of Fluoride from Aqueous Solution by Mg-Al-Zr Triple-Metal Composite. *Chem. Eng. J.* **2017**, *322*, 246–253, doi:10.1016/j.cej.2017.03.155.
5. Maliyekkal, S.M.; Sharma, A.K.; Philip, L. Manganese-Oxide-Coated Alumina: A Promising Sorbent for Defluoridation of Water. *Water Res.* **2006**, *40*, 3497–3506, doi:10.1016/j.watres.2006.08.007.
6. Kang, D.; Yu, X.; Ge, M. Morphology-Dependent Properties and Adsorption Performance of CeO2 for Fluoride Removal. *Chem. Eng. J.* **2017**, *330*, 36–43, doi:10.1016/j.cej.2017.07.140.
7. Ma, W.; Zhao, N.; Yang, G.; Tian, L.; Wang, R. Removal of Fluoride Ions from Aqueous Solution by the Calcination Product of Mg–Al–Fe Hydrotalcite-like Compound. *Desalination* **2011**, *268*, 20–26, doi:10.1016/j.desal.2010.09.045.
8. Patnaik, P.C.; Swain, S.K.; Patel, S.B.; Patnaik, T.; Muller, F.; Delpeux-Ouldriane, S.; Das, S.; Dey, R.K. Kinetics and Thermodynamics of Defluoridation of Drinking Water Using High Performance Hybrid Zirconium (IV)-Hexamethylenediamine: A Comparative Aspect with Ion-Exchanger Amorphous Zirconium (IV) Phosphate. *Surf. Interfaces* **2018**, *13*, 22–32, doi:10.1016/j.surfin.2018.07.001.
9. Vences-Alvarez, E.; Velazquez-Jimenez, L.H.; Chazaro-Ruiz, L.F.; Diaz-Flores, P.E.; Rangel-Mendez, J.R. Fluoride Removal in Water by a Hybrid Adsorbent Lanthanum–Carbon. *J. Colloid Interface Sci.* **2015**, *455*, 194–202, doi:10.1016/j.jcis.2015.05.048.
10. Shang, Y.; Xu, X.; Gao, B.; Yue, Q. Highly Selective and Efficient Removal of Fluoride from Aqueous Solution by ZrLa Dual-Metal Hydroxide Anchored Bio-Sorbents. *J. Clean. Prod.* **2018**, *199*, 36–46, doi:10.1016/j.jclepro.2018.07.162.
11. Chen, L.; Zhang, K.-S.; He, J.-Y.; Xu, W.-H.; Huang, X.-J.; Liu, J.-H. Enhanced Fluoride Removal from Water by Sulfate-Doped Hydroxyapatite Hierarchical Hollow Microspheres. *Chem. Eng. J.* **2016**, *285*, 616–624, doi:10.1016/j.cej.2015.10.036.
12. Minju, N.; Venkat Swaroop, K.; Haribabu, K.; Sivasubramanian, V.; Senthil Kumar, P. Removal of Fluoride from Aqueous Media by Magnesium

Oxide-Coated Nanoparticles. *Desalination Water Treat.* **2015**, *53*, 2905–2914, doi:10.1080/19443994.2013.868837.